

Fast and accurate predictions of covalent bonds in chemical space

K. Y. Samuel Chang,¹ Stijn Fias,² Raghunathan Ramakrishnan,¹ and O. Anatole von Lilienfeld^{1,*}

¹*Institute of Physical Chemistry and National Center for Computational Design and Discovery of Novel Materials (MARVEL),
Department of Chemistry, University of Basel, 4056 Basel, Switzerland*

²*General Chemistry (ALGC), Free University Brussels (VUB), Pleinlaan 2, 1050 Brussel, Belgium*

(Dated: September 24, 2018)

We assess the predictive accuracy of perturbation theory based estimates of changes in covalent bonding due to linear alchemical interpolations among molecules. We have investigated σ bonding to hydrogen, as well as σ and π bonding between main-group elements, occurring in small sets of iso-valence-electronic molecular species with elements drawn from second to fourth rows in the p -block of the periodic table. Numerical evidence suggests that first order estimates of covalent bonding potentials can achieve chemical accuracy if (i) the alchemical interpolation is vertical (fixed geometry), (ii) involves molecules containing elements in the third and fourth row of the periodic table, and (iii) a reference geometry is optimized. In this case, changes in the bonding potential become near-linear in coupling parameter, resulting in analytical predictions with very high accuracy (~ 1 kcal/mol). Second order estimates deteriorate the prediction. If initial and final molecules differ not only in composition but also in geometry, all estimates become substantially worse, with second order being slightly more accurate than first order. The independent particle approximation to the second order perturbation performs poorly when compared to the coupled perturbed or finite difference approach. Taylor series expansions up to fourth order of the potential energy curve of highly symmetric systems indicate a finite radius of convergence, as illustrated for the alchemical stretching of H_2^+ . Numerical results are presented for (i) covalent bonds to hydrogen in 12 molecules with 8 valence electrons (CH_4 , NH_3 , H_2O , HF , SiH_4 , PH_3 , H_2S , HCl , GeH_4 , AsH_3 , H_2Se , HBr); (ii) main-group single bonds in 9 molecules with 14 valence electrons (CH_3F , CH_3Cl , CH_3Br , SiH_3F , SiH_3Cl , SiH_3Br , GeH_3F , GeH_3Cl , GeH_3Br); (iii) main-group double bonds in 9 molecules with 12 valence electrons (CH_2O , CH_2S , CH_2Se , SiH_2O , SiH_2S , SiH_2Se , GeH_2O , GeH_2S , GeH_2Se); (iv) main-group triple bonds in 9 molecules with 10 valence electrons (HCN , HCP , HCAs , HSiN , HSiP , HSiAs , HGeN , HGeP , HGeAs); (v) H_2^+ single bond with 1 electron.

I. INTRODUCTION

Solving Schrödinger’s time independent equation for the unperturbed electronic ground-state within the Born-Oppenheimer approximation yields the potential energy surface (PES) of *any* molecule as a function of nuclear charges $\{Z_I\}$ (stoichiometry), nuclear positions $\{\mathbf{R}_I\}$ (geometry), and number of electrons N (molecular charge).^{1,2} The PES plays a fundamental role in chemistry and elsewhere because many properties can be derived from it. While one can study efficient ways of predicting the PES of single compounds^{3–5} efficient estimates of PES of ensembles of molecules are more useful (and challenging) in the context of virtual compound design efforts.^{6–10} These efforts typically attempt to search chemical compound space (CCS) spanned by $\{\{Z_I\}, \{\mathbf{R}_I\}, N\}$ ^{11,12} for novel materials with desirable properties. As such, accurate yet efficient quantum mechanics (QM) based PES estimates hold the key for successful rational compound design applications.^{6,7,13–15} While many inexpensive semi-empirical QM methods are available, for this study we restrict ourselves to first principles in the spirit of Refs.^{12,16–22} More specifically, we investigate the application of “alchemical” coupling to the problem of efficiently estimating the PES of new molecules using Taylor series expansions in CCS, rather than empiricism.

The alchemical coupling approach can be related to

grand-canonical ensemble theory (Widom insertion)^{23–25}, and has been well established for empirical force-field based molecular dynamics studies.^{26–30} Using QM, alchemical changes are less common despite E. B. Wilson’s early proposal of variable Z , back in 1962.³¹ Within QM, any two iso-electronic molecules in CCS can be coupled “alchemically” through interpolation of their external potentials. Here, we have investigated if alchemical predictions can be used to model the PES of covalent bonds occurring in small closed-shell molecules made up from main group elements. We have limited ourselves to covalent hydrogen bonds, as well as single, double, and triple bonds in molecules with no more than 14 valence electrons. We present and discuss numerical evidence for the following set of observations: First order Taylor-expansions of covalent bonding potentials can reach chemical accuracy (~ 1 kcal/mol) if two conditions are met. Firstly, the alchemical change has to be “vertical”, meaning that initial reference molecule as well as final target molecule have to possess the same number of atoms located at the exact same positions. Secondly, all elements involved in the alchemical change, i.e. all $\{Z_I\}$ destined to vary, have to occur late in the periodic table. Second order Taylor-expansion based predictions are less accurate than first order predictions if these conditions are met. If reference and target molecule have different geometries, the predictive power of the first order Taylor expansion substantially deteriorates, while second order estimates based on coupled perturbed Kohn-Sham equa-

tions offer some improvement, however, without reaching chemical accuracy. Second order estimates based on the independent particle approximation result in Taylor expansion estimates that are even worse than first order estimates. For highly symmetrical alchemical changes, such as the dissociation of H_2^+ , a finite radius of convergence is found.

In Sec. II we briefly summarize the framework of alchemical derivatives within Hartree-Fock and density functional theory (DFT) as well as our notations. Numerical estimations of covalent bond stretching of small molecules are presented and discussed in Sec. III: Extending previous work on alchemical perturbation,^{19,20,32} we discuss alchemical energy derivatives with respect to vertical transmutation, interpolating only the identity of the atoms while keeping the geometry fixed. Estimates of single, double and triple bonds are included as an application. We also report numerical results for alchemical stretching of chemical bonds using non-vertical transmutations. Finally, conclusions are drawn in Sec. IV.

II. METHOD

A. Taylor expansion in CCS

A Taylor expansion in CCS can be constructed with the exclusive knowledge acquired by solving Schrödinger's equation for some reference molecule, with Hamiltonian H_R ,

$$E(\Delta\lambda) = E_R + \Delta\lambda\partial_\lambda E_\lambda \Big|_{\lambda=0} + \frac{\Delta\lambda^2}{2}\partial_\lambda^2 E_\lambda \Big|_{\lambda=0} + \dots \quad (1)$$

Derivatives of the total potential energy can be obtained by coupling a reference Hamiltonian to some target Hamiltonian, H_T , such that H_λ transforms H_R into H_T

$$H_\lambda = (1 - \lambda)H_R + \lambda H_T, \quad (2)$$

as the coupling parameter λ goes from 0 to 1. And consequently, $\partial_\lambda^m E_\lambda = \partial_\lambda^m \langle H_\lambda \rangle$, with $\partial_\lambda H_\lambda = H_T - H_R = H'$ being the alchemical perturbing Hamiltonian. If these derivatives can be computed, E_T can be estimated according to Eq. (1) by setting $\Delta\lambda = 1$. Note that we couple reference and target systems in a linear and global fashion. This is an arbitrary choice, non-linear and local interpolation functions could have been chosen just as well. In fact, in Ref. 20, an empirical quadratic interpolation function is found to yield superior results for first order predictions of highest occupied molecular orbital (HOMO) eigenvalues. In this study of alchemical changes of covalent bonding, we begin with linear and global interpolations, future work might deal with alternative functions.

Given a pair of isoelectronic reference/target systems, described by $\{\{Z_I^R\}, \{\mathbf{R}_I^R\}, N\}$ and $\{\{Z_I^T\}, \{\mathbf{R}_I^T\}, N\}$ respectively, one can couple the two systems such that certain Z_I^R and Z_I^T are paired. Note that Z_I^R or Z_I^T can

be scaled down to/up from zero if the number of atoms in one molecule is smaller. Under isoelectronic conditions, the λ -dependent terms in the coupling Hamiltonian (Eq. (2)) are the electron-nucleus and nucleus-nucleus interaction operators,

$$\begin{aligned} v_\lambda(\mathbf{r}) &= \sum_I^{N_I} \left(-\frac{(1-\lambda)Z_I^R}{|\mathbf{r} - \mathbf{R}_I^R|} - \frac{\lambda Z_I^T}{|\mathbf{r} - \mathbf{R}_I^T|} \right), \\ V_\lambda &= \sum_{I < J}^{N_I} \left(\frac{(1-\lambda)Z_I^R Z_J^R}{|\mathbf{R}_I^R - \mathbf{R}_J^R|} + \frac{\lambda Z_I^T Z_J^T}{|\mathbf{R}_I^T - \mathbf{R}_J^T|} \right). \end{aligned} \quad (3)$$

Since different pairing schemes result in different $v_\lambda(\mathbf{r})$ and V_λ , it is obvious that the alchemical perturbation is alignment dependent. To investigate the behaviour of higher order corrections and the effects of varying geometry/stoichiometry, we neglect all relaxation effects for vertical iso-valence-electronic changes (see Sec. II G).

B. First order derivative

The first order derivative of the energy with respect to an alchemical interpolation parameter connecting *any* two iso-electronic molecules, can be computed according to the Hellmann-Feynman theorem,³³ as shown for molecular HOMO eigenvalues,²⁰

$$\partial_\lambda E_\lambda = \langle \partial_\lambda H_\lambda \rangle_\lambda = \int d\mathbf{r} \rho_\lambda(\mathbf{r}) \partial_\lambda v_\lambda(\mathbf{r}) + \partial_\lambda V_\lambda, \quad (4)$$

where $\rho_\lambda(\mathbf{r})$ denotes the electron density, dependent on λ . At $\lambda = 0$ we have $\rho_\lambda(\mathbf{r}) = \rho_R(\mathbf{r})$, which is independent of the target system. As such, the first order derivative can be calculated with a single reference density and without additional self-consistent field (SCF) calculation for *any* target system. In several circumstances, Taylor expansion estimates using first order alchemical derivatives have shown good accuracy for the rapid prediction of properties throughout CCS.^{12,21,32,34,35} In general, however, first order derivatives might not be sufficient. Taking higher order derivatives into account might offer higher accuracy, assuming Eq. (1) converges rapidly.

C. Second order derivative

Differentiation of Eq. (4), based on linear interpolated Hamiltonian in Eq. (2), yields

$$\partial_\lambda^2 E_\lambda = \int d\mathbf{r} (\partial_\lambda \rho(\mathbf{r})) (\partial_\lambda v_\lambda(\mathbf{r})), \quad (5)$$

requiring the density response due to the alchemical perturbation. Again, at $\lambda = 0$ this amounts to the density response of the reference system. Evaluation of Eq. (5) implies a differing density response for each target system. We have considered three approximations to $\partial_\lambda \rho$

including second order perturbation theory with independent particle approximation³⁶ (IPA), coupled perturbed (CP) approaches,^{37,38} as well as finite difference approximation (FD). Note that Eq. (5) can be rewritten as $\partial_\lambda^2 E = \int d\mathbf{r}d\mathbf{r}'(\partial_\lambda v(\mathbf{r}))(\partial_\lambda v(\mathbf{r}'))\frac{\delta^2 E}{\delta v(\mathbf{r})\delta v(\mathbf{r}'')}$, where $\frac{\delta^2 E}{\delta v(\mathbf{r})\delta v(\mathbf{r}'')} = \chi(\mathbf{r}, \mathbf{r}'')$ is the static linear response function or susceptibility, well established within conceptual DFT^{39–44}.

Perturbation theory provides ways to estimate $\partial_\lambda \rho_\lambda(\mathbf{r})$.⁴⁵ Within IPA^{36,46,47}, the static density response for a close-shell system is approximated by

$$\begin{aligned} \partial_\lambda \rho_\lambda(\mathbf{r}) \approx & -4 \sum \phi_i(\mathbf{r})\phi_a(\mathbf{r}) \\ & \times \int d\mathbf{r}' \frac{\phi_i(\mathbf{r}')\phi_a(\mathbf{r}')}{\varepsilon_a - \varepsilon_i} \partial_\lambda v_\lambda(\mathbf{r}'), \end{aligned} \quad (6)$$

where $\{\phi_i, \varepsilon_i\}$ denote the i^{th} occupied molecular orbitals (MOs) and their eigenvalues, while $\{\phi_a, \varepsilon_a\}$ denote the a^{th} unoccupied counterparts. IPA neglects the influence of the alchemical perturbation on the Hartree and exchange-correlation (xc) potentials.^{38,42} Note that Eq. (6) becomes numerically exact for 1-electron system with converged basis set within Hartree-Fock approximation, because of the absence of Coulomb and xc interaction between electrons.

Recently, Yang, Cohen, De Proft and Geerlings derived an expression of the density response that also includes the dependence of Coulomb and xc potential,³⁷ the CP approach,⁴⁴

$$\begin{aligned} \partial_\lambda \rho_\lambda(\mathbf{r}) = & -4 \sum_{ij} \sum_{ab} \phi_i(\mathbf{r})\phi_a(\mathbf{r}) \\ & \times (\mathbf{M}^{-1})_{ia,jb} \int d\mathbf{r}' \phi_j(\mathbf{r}')\phi_b(\mathbf{r}') \partial_\lambda v_\lambda(\mathbf{r}'), \end{aligned} \quad (7)$$

where the matrix elements of \mathbf{M} are

$$\begin{cases} \mathbf{M}_{ia,jb} = (\varepsilon_a - \varepsilon_i)\delta_{ij}\delta_{ab} + 4\mathbf{J}_{ia,jb} + 4\mathbf{X}_{ia,jb}, \\ \mathbf{J}_{ia,jb} = \int d\mathbf{r}d\mathbf{r}' \frac{\phi_i(\mathbf{r})\phi_a(\mathbf{r})\phi_j(\mathbf{r}')\phi_b(\mathbf{r}')}{|\mathbf{r} - \mathbf{r}'|}, \\ \mathbf{X}_{ia,jb} = \int d\mathbf{r}d\mathbf{r}' \phi_i(\mathbf{r})\phi_a(\mathbf{r})\phi_j(\mathbf{r}')\phi_b(\mathbf{r}') \\ \quad \times \left(\frac{\delta^2 E_{xc}}{\delta \rho(\mathbf{r})\delta \rho(\mathbf{r}')} \right). \end{cases} \quad (8)$$

In the limit of $\mathbf{J}_{ia,jb} \rightarrow 0$ and $\mathbf{X}_{ia,jb} \rightarrow 0$, Eq. (6) and Eq. (7) are equivalent.

Alternatively, one can also introduce an explicit small perturbation and converge the new density at $\Delta\lambda \ll 1$. The density response can then be estimated via FD, $\partial_\lambda \rho(\mathbf{r}) \approx \frac{\rho_{\Delta\lambda}(\mathbf{r}) - \rho_{\text{R}}(\mathbf{r})}{\Delta\lambda}$. In practice, instead of starting the SCF for the perturbed system from atom based initial guesses, we restart with $\rho_{\text{R}}(\mathbf{r})$ resulting in convergence within few SCF steps.

D. Higher order derivatives

Møller-Plesset (MP) perturbation theory^{48,49} is used to estimate correlation energy corrections based on converged Hartree-Fock results. The derivation of higher order corrections in MP theory are equivalent to the m^{th} order alchemical derivative. Here, instead of the two-particle operator for electron-electron interaction as perturbation in MP theory, the alchemical perturbation operator $H_T - H_R$ can be used. Within IPA, the MP formula can be directly applied to obtain any m^{th} order derivative.

E. Predicting changes in covalent bonds

For the study of covalent bonds we focus on the changes in binding potential due to alchemical coupling. We consider the difference in total potential energy between two bounded atoms at two arbitrary interatomic distances d and d_0 ,

$$\Delta E(d, d_0) = E(d) - E(d_0). \quad (9)$$

If, for example, d_0 is large and d is the geometry minimum, ΔE becomes the bond dissociation energy. We are interested in changes of $\Delta E(d, d_0)$ as a function of d due to alchemical changes for a fixed d_0 . More specifically, we couple a reference to target system via the corresponding Hamiltonians yielding expectation values as a function of λ ,

$$\begin{aligned} \Delta E_\lambda(d, d_0) = & E_\lambda(d) - E_\lambda(d_0) \\ = & \langle H_R(d) + \lambda(H_T(d) - H_R(d)) \rangle \\ & - \langle H_R(d_0) + \lambda(H_T(d_0) - H_R(d_0)) \rangle. \end{aligned} \quad (10)$$

As λ goes from zero to one, the two components in Eq. (9) change from reference ($E_{\text{R}}(d), E_{\text{R}}(d_0)$) to target ($E_{\text{T}}(d), E_{\text{T}}(d_0)$) compound. The truncated Taylor expansion based estimate of the target compound's potential is then obtained via,

$$\begin{aligned} \Delta E_{\text{T}}(d, d_0) \approx & \Delta E_{\text{T}}^{(m)}(d, d_0) = \Delta E_{\text{R}}(d, d_0) \\ & + \sum_{k=1}^m \frac{1}{k!} \partial_\lambda^k \Delta E_\lambda(d, d_0), \end{aligned} \quad (11)$$

where the superscript m stands for Taylor expansion with m terms, as a function of bond-length d for vertical alchemical changes. Since ΔE_{T} is the property of interest, the subscript T , λ , and the dependency of d_0 will be omitted for the rest of this work, unless otherwise noted. In this study we investigated orders up to $m = 4$ for the stretching of H_2^+ , and up to $m = 2$ for all other molecules.

For a fixed d_0 , first and second order estimation are

$$\Delta E^{(1)}(d) = (E_R(d) + \partial_\lambda E_\lambda(d)) - (E_R(d_0) + \partial_\lambda E_\lambda(d_0)), \quad (12)$$

$$\Delta E^{(2)}(d) = (E_R(d) + \partial_\lambda E_\lambda(d) + \frac{1}{2}\partial_\lambda^2 E_\lambda(d)) - (E_R(d_0) + \partial_\lambda E_\lambda(d_0) + \frac{1}{2}\partial_\lambda^2 E_\lambda(d_0)). \quad (13)$$

Since d and d_0 in Eq. (9) are arbitrary, one can infer the binding curve via scanning d for any fixed d_0 . The predictive power, however, happens to dependent on d_0 . For this reason, we optimize d_0 such that the integrated error in dissociation region is minimal. As shown in Fig. 5, an empirical linear relationship exists between equilibrium bond length of target molecule d_{eq}^T , and d_{opt}

$$d_{\text{opt}} \approx 0.76 d_{\text{eq}}^T + 0.97 \text{ \AA}. \quad (14)$$

d_0 is determined according to Eq. (14) for all vertical changes. If d_{eq}^T is not known it can easily be estimated with semi-empirical quantum chemistry methods. For non-vertical changes, we fix $d_0 = d_{\text{eq}}$ to the equilibrium distance in the reference molecule, resulting in $\Delta E^{(m)}(d_{\text{eq}}) = 0$. Eqs. (12, 13) become

$$\Delta E^{(1)}(d) = (E_R(d) + \partial_\lambda E_\lambda(d)) - (E_R(d_{\text{eq}}) + \partial_\lambda E_\lambda(d_{\text{eq}})), \quad (15)$$

$$\Delta E^{(2)}(d) = (E_R(d) + \partial_\lambda E_\lambda(d) + \frac{1}{2}\partial_\lambda^2 E_\lambda(d)) - (E_R(d_{\text{eq}}) + \partial_\lambda E_\lambda(d_{\text{eq}}) + \frac{1}{2}\partial_\lambda^2 E_\lambda(d_{\text{eq}})).$$

F. Error measures

For bond lengths, we quantify the predictive power of the Taylor expansions by evaluating the deviation of prediction from the DFT bond length $\Delta d_{\text{eq}} = d_{\text{eq}}^{(m)} - d_{\text{eq}}$, where $d_{\text{eq}}^{(m)}$ stands for the predicted equilibrium distance of $\Delta E^{(m)}$. We calculate the deviation of the predicted energy at $d_{\text{eq}}^{(m)}$ from the DFT energy at the DFT minimum, $\Delta E_{\text{eq}} = \Delta E^{(m)}(d_{\text{eq}}^{(m)}) - \Delta E(d_{\text{eq}})$. The deviation in harmonic vibration frequency, $\Delta\omega = \omega^{(m)} - \omega$, of the stretching bond is also included in order to quantify the accuracy of the stiffness of the predicted binding potential. The vibration frequency is computed from the curvature of cubic spline interpolated binding potential, $\omega = \frac{1}{2\pi} \sqrt{\frac{k_{\text{eq}}}{\mu}}$ where $k_{\text{eq}} = \partial_d^2 \Delta E(d_{\text{eq}})$ and μ is the reduced mass. Finally, we measure the integrated error (IE) for the dissociative tail, defined as

$$\text{IE} = \frac{1}{|d_{\text{max}} - d_{\text{eq}}^{(m)}|} \int_{d_{\text{eq}}^{(m)}}^{d_{\text{max}}} dx |\Delta E^{(m)}(x) - \Delta E(x)|, \quad (16)$$

for vertical iso-valence-electronic changes. Note that while in principle one would like $d_{\text{max}} \rightarrow \infty$, d_{max} has

been set to correspond roughly to the inflection point, due to the issues of a single reference such as DFT method for describing covalent bond-dissociation. This shortcoming is also evident from comparison of DFT to CCSD(T) curves shown in Fig. 3.

Note that this aspect is irrelevant for the alchemical predictions: If a more reliable reference method had been used the error integration could easily be expanded to include the entire dissociative tail. These four quantities provide a numerical indication of how good a prediction is. For a perfect prediction one would expect $(\Delta E_{\text{eq}}, \Delta d_{\text{eq}}, \Delta\omega, \text{IE}) = (0, 0, 0, 0)$. Note that we compare the predictions to DFT. This is an arbitrary choice, any other QM method could have been applied just as well.

G. Computational details

Alchemical interpolations of molecules containing elements from different rows in the periodic table can still be iso-electronic if effective core or pseudo potentials (PPs) are used, resulting in a constant number of valence electrons¹². For example, one can couple carbon to silicon using just four valence electrons. Non-local PPs are widely used to mimic the presence of core electrons in atoms⁵⁰, and are amenable to the tuning of a wide range of properties including dispersion forces, band-gap, or vibrational frequencies^{51–53}. The non-local external potential $v_\lambda(\mathbf{r})$ in Eq. (3) then becomes

$$v_\lambda(\mathbf{r}, \mathbf{r}') = \sum_I^{N_I} \left((1 - \lambda) v_I^R(\mathbf{r}, \mathbf{r}') + \lambda v_I^T(\mathbf{r}, \mathbf{r}') \right), \quad (17)$$

where v_I^R and v_I^T are PPs for Z_I^R and Z_I^T respectively. Note that $v_\lambda(\mathbf{r}, \mathbf{r}')$ in Eq. (17) and $v_\lambda(\mathbf{r})$ in Eq. (3) result in different coupling Hamiltonians, and therefore different λ -dependencies of the energy and its derivatives.

All results have been obtained within the Born-Oppenheimer approximation, where nuclei are clamped, nuclear repulsion V_λ is decoupled from the electronic wavefunction, and is added as a geometry- and λ -dependent constant to the electronic energy. Nuclear-nuclear repulsion energy is computed automatically by most QM codes. However, it must be removed and recomputed independently for V_λ according to Eq. (3) to avoid self-repulsion between transmutating atoms. Throughout the present study, standard atomic and plane-wave basis functions, linearly interpolated PPs, as well as the PBE xc potential⁵⁴ within KS-DFT is used. The scanning of $0.5 \text{ \AA} \leq d \leq 3.0 \text{ \AA}$ is carried out with increments $\Delta d = 0.1 \text{ \AA}$. For each prediction order m , $\Delta E^{(m)}(d)$ are interpolated with cubic splines, from which the stiffness $\partial_d^2 \Delta E^{(m)}(d_{\text{eq}}^{(m)}) = k_{\text{eq}}$ is computed. All density volumetric data is printed into **Gaussian** CUBE files, from which integrated density slices are calculated.

1. Details for vertical iso-valence-electronic changes

Numerical results for vertical iso-valence-electronic alchemical changes (discussed in Sec. III A and III B) have been obtained with CPMD⁵⁵, a plane wave basis with 100 Ry cutoff, and Goedecker PPs.^{56–58} The periodic supercell size is $20 \times 15 \times 15 \text{ \AA}^3$, and one heavy atom is fixed at $(7.5 \text{ \AA}, 7.5 \text{ \AA}, 7.5 \text{ \AA})$ while the stretching atom shifts along $+x$ -axis. For each geometry, heavy atoms are mutated to other elements in the same column of the periodic table while all H are fixed at the same location as in the reference compound.

Since Eq. (17) is a non-local operator, Eqs. (4) and (5) need to be converted to wavefunction expressions. The first order derivative for the Hamiltonian $H_{R \rightarrow T}$ is evaluated using RESTART files in which the reference compound’s density and wavefunctions have been stored: $\partial_\lambda E = \langle \partial_\lambda H \rangle_R = E_T[\rho_R] - E_R[\rho_R]$. And the second order derivative is evaluated correspondingly relying on FD, $\partial_\lambda^2 E \approx \frac{\langle \partial_\lambda H \rangle_{\Delta\lambda} - \langle \partial_\lambda H \rangle_R}{\Delta\lambda}$, with $\Delta\lambda = 0.05$. Wavefunctions of reference compound are used for $\Delta E^{(1)}$, while $\Delta E_{\text{FD}}^{(2)}$ is evaluated by FD with linearly interpolated PPs parameter.

Coupled-cluster results (CCSD(T)) obtained for HCl and HBr have been computed using Gaussian09⁵⁹ in aug-cc-pVTZ-⁶⁰ basis, and default input parameters.

2. Details for non-vertical iso-electronic changes

Numerical results for non-vertical iso-electronic alchemical changes have been obtained using atom centered basis-sets. Restricted open-shell Hartree-Fock calculations have been carried out using Cartesian aug-cc-pVTZ basis set⁶⁰ for H_2^+ (Discussed in Sec. III D 1). Eq. (6) and higher order derivatives are evaluated analytically by Gaussian expansion of MOs. Reference geometry is first relaxed by Gaussian09⁵⁹ and the converged MO coefficients are extracted to evaluate orbital integrals. NWChem⁶¹ is used to scan ΔE as a function of λ in Fig. 6(d) along alchemical path with discretization $\Delta\lambda = 0.01$. It is done by reassigning nuclear charges in the system.

Non-vertical alchemical changes in 10-electron molecules (discussed in Sec. III D 2) have been calculated using the uncontracted Cartesian Def2TZVP basis set⁶². Uncontracted neon basis is used for second row heavy atoms. Additional hydrogen basis functions are placed along the stretching pathway, from $d = 0.5 \text{ \AA}$ to $d = 3.0 \text{ \AA}$ in increments $\Delta d = 0.1 \text{ \AA}$. All systems with integer nuclear charges have been calculated using Gaussian09⁵⁹ while systems with fractional nuclear charges have been calculated using NWChem⁶¹ with discretization $\Delta\lambda = 0.01$. For each $0 \leq \lambda \leq 1$, the atomic density for SCF initial guess iterates through {C, N, O, F, Ne} to ensure convergence. In all Gaussian and NWChem calculations we used Cartesian/Real spherical

harmonic basis functions.

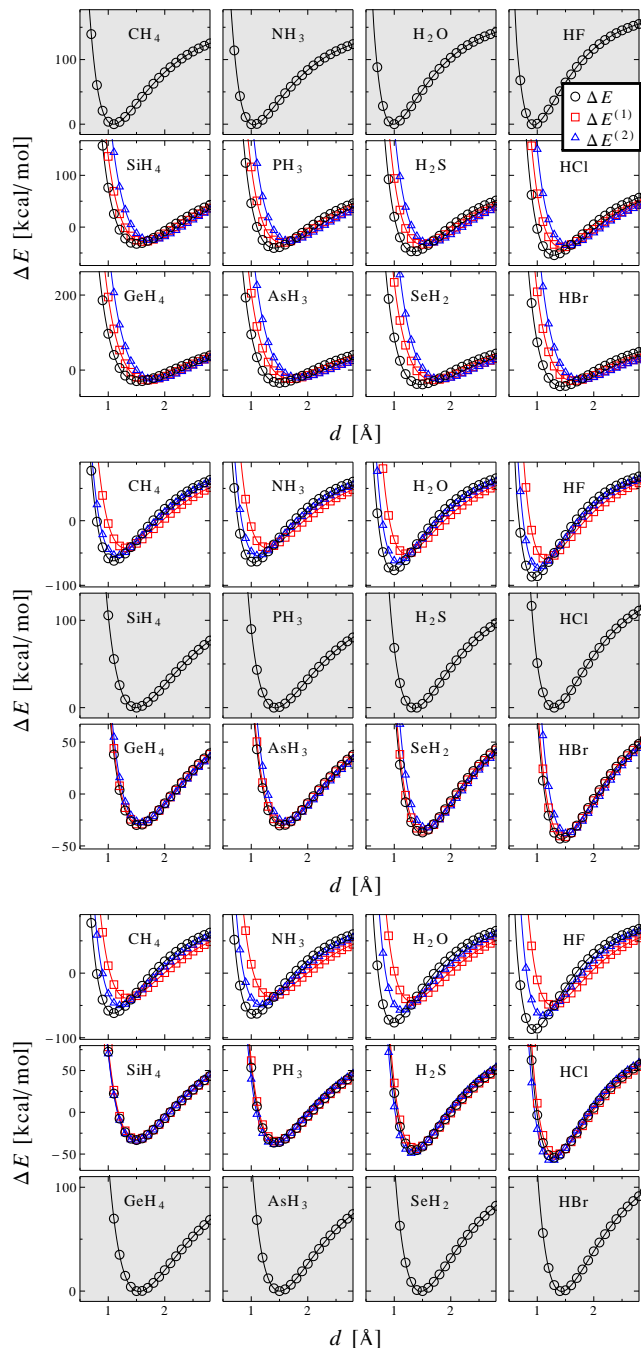


FIG. 1. ΔE is shown as a function of d in Eq. (11). White background panels: True (black circles), first (red squares) and second (blue triangles) order predictions of changes in the covalent bond of hydrogen due to vertical alchemical interpolations. Gray background panels: The true potentials of the reference compounds employed for the predictions for the first and second order predictions.

III. RESULTS AND DISCUSSIONS

A. Vertical iso-valence-electronic changes of X-H

1. Predicted potentials

Using Taylor expansions binding potentials have been estimated for covalent bonds involving hydrogen (X-H) for the following 12 molecules with 8 valence electrons: CH₄, NH₃, H₂O, HF (second period); SiH₄, PH₃, H₂S, HCl (third period); and GeH₄, AsH₃, H₂Se, HBr (fourth period). Numerical results for vertical first (red) and second (blue) order truncated Taylor series estimates feature in Fig. 1. They measure the change in X-H binding energy as one goes from reference to target compound.

We first note that the entire potential is reproduced in semi-quantitative fashion for all combinations of reference/target molecules. The precise predictive power strongly depends on the choice of reference/target molecule pair, on the choice of d_0 , and on the expansion going up to first or second order. First order estimates among molecules with elements from third or fourth row are very accurate (See Fig. 1, bottom and mid row in mid and bottom panel, respectively). By contrast, predicting, or starting with, second row elements consistently yields worse results. Inclusion of second order corrections does not necessarily lead to improved performance. Second order truncated Taylor series estimates only yield more accurate predictions than first order when the reference molecule contains heavier elements than the target molecule. For example, if we predict HF using HBr as a reference, the second order prediction is more accurate than first order. Making the inverse prediction (i.e. HBr from HF), however, first order is more accurate than second order.

The performance of truncated Taylor series dramatically varies depending on the choice of the d_0 value. The top panel in Fig. 2 illustrates this for $\Delta E(2\text{\AA}, d_0)$ for HF \rightarrow HBr as a function of λ , once with $d_0 = 0.94\text{\AA}$ —the equilibrium bond length of HF— and once with $d_0 = 1.57\text{\AA}$, a value for d_0 which happens to linearize ΔE in λ . While the coupling path of total energies is hardly distinguishable for $E(2\text{\AA})$, $E(1.57\text{\AA})$, and $E(0.94\text{\AA})$, ΔE is strongly dependent on the choice of d_0 . By choosing $d_0 = 1.57\text{\AA}$, $\Delta E(2\text{\AA}, 1.57\text{\AA})$ in Eq. (10) becomes nearly linear, while plotting $\Delta E(2\text{\AA}, 0.94\text{\AA})$ reveals substantial curbing. This is why, when choosing the right d_0 , first order predictions of ΔE can be very predictive.

The top panel in Fig. 2 also explains why second order estimates can be worse than first order, and why this changes for the reverse coupling: On the side of the lighter element ($\lambda \rightarrow 0$), a weak convexity is noticeable in ΔE (blue line), despite the overall concavity of the path. The presence of inflection points will always lead to a deterioration of second order predictions, resulting in a more accurate first order estimate. On the other side ($\lambda \rightarrow 1$), no such inflection point exists and the second order term results in the expected improvement of

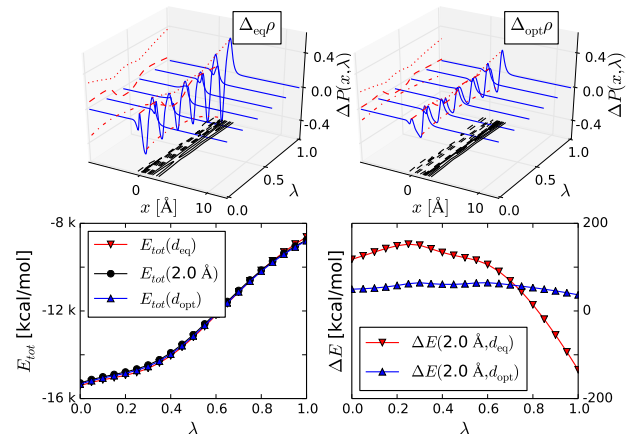


FIG. 2. Alchemical coupling of HF ($\lambda = 0$) to HBr ($\lambda = 1$). TOP panel: E and ΔE where $d_{\text{eq}} = 0.94\text{\AA}$ (red) denotes the equilibrium bond length of reference molecule HF, and $d_{\text{opt}} = 1.57\text{\AA}$ (blue) linearizes ΔE . BOTTOM panel: Integrated valence electron density difference slices between H-X at $d = 2\text{\AA}$ and at d_{opt} and d_{eq} , respectively, $\Delta P_\lambda(x) = \int dydz[\rho_\lambda(\mathbf{r}, d) - \rho_\lambda(\mathbf{r}, d_0)]$. Dependence on λ is shown for the same vertical interpolations, Left and Right corresponding to the non-linear (red) and linearized (blue) ΔE curves in right-hand TOP panel. Density changes at heavy atom and hydrogen positions are highlighted as red dashed and dotted/dash-dotted lines, respectively.

the prediction. For the other compound pairs shown in Fig. 1 similar observations can be made for the attractive part of the bonding potential (see also $\Delta E(2\text{\AA}, d_0)$ curves in supplementary materials). We have found that the inflection point near $\lambda = 0$ occurs only when the reference molecule has the lighter element. Conversely, no inflection point has been observed for atoms transmutating upward the column. We believe that this behaviour is due to the specifics of the employed PPs. Future studies will show why this is the case, and if similar trends hold for other PPs.

2. Integrated error

Prediction errors for energy minima, equilibrium bond lengths, force constants, and integrated error in dissociation region (calculated as described in Sec. IIF) have been obtained for all predictions in Fig. 1, and are listed in Table. I. The results lend quantitative support for the observations articulated above. In particular, the results suggest that chemical accuracy can be obtained when using first order Taylor series based estimates among compounds containing third and fourth row elements. Second order based predictions are *always* worse except when a molecule with heavier element is used as a reference to predict a molecule with lighter one, for example HBr \rightarrow HF.

The best prediction performance is found for first order based estimates using reference molecules containing third row elements ($n_R = 3$) in order to predict target molecules made up of fourth row elements ($n_T = 4$). The overall average deviation from reference bonding potential energies and integrated error are ~ 2.5 kcal/mol. Corresponding predictions of equilibrium distances deviate at most by 0.03\AA , and the vibration frequencies deviate no more than 32 cm^{-1} . Second order estimates for the same third and fourth row combinations give slightly worse results. The worst predictions are found if the

coupled molecules skip a row, *i.e.* involve elements from second and fourth row—for first as well as second order truncated Taylor expansions. This is not surprising as the central atom’s electron density must accommodate the most severe contractions/expansions for such interpolations. Moreover, second order overcorrections can also be found (Table. I) whenever molecules containing fourth row elements are used to predict molecules containing third row elements: Both, predicted energy minimum and equilibrium bond length, show negative deviations.

TABLE I. Error measures for first (left) and second (right) order predictions of vertical iso-valence-electronic alchemical changes of covalent bond potentials in X-H \rightarrow A-H. The compound pairs are arranged in the same way as in Fig. 1, *i.e.* each box corresponds to an unshaded panel containing a predicted potential. Unit are [kcal/mol] for ΔE_{eq} and IE, [\AA] for Δd_{eq} , and $\Delta\omega$ in [cm^{-1}]. Avg corresponds to averaged signed error for each row with corresponding unit. Periods of X and A are denoted by their respective primary quantum number $n_R, n_T = \{2, 3, 4\}$. IV, V, VI, VII represent the columns of X and A in the periodic table.

$\Delta E^{(1)}, n_R = 2$						
n_T		IV.	V.	VI.	VII.	Avg
$n_T = 3$	ΔE_{eq}	10.55	17.19	22.16	24.05	18.49
	Δd_{eq}	0.12	0.14	0.15	0.15	0.14
	$\Delta\omega$	-46.9	-109.6	-188.5	-213.7	-139.7
	IE	13.01	20.00	27.43	30.18	22.65
$n_T = 4$	ΔE_{eq}	10.76	19.97	23.77	25.74	20.06
	Δd_{eq}	0.15	0.20	0.24	0.21	0.20
	$\Delta\omega$	-22.8	-137.8	-164.1	-196.8	-130.3
	IE	13.19	28.19	36.84	39.42	29.41

$\Delta E^{(1)}, n_R = 3$						
n_T		IV.	V.	VI.	VII.	Avg
$n_T = 2$	ΔE_{eq}	32.90	36.17	41.62	44.65	38.84
	Δd_{eq}	0.21	0.23	0.23	0.22	0.22
	$\Delta\omega$	-308.4	-373.8	-527.3	-575.0	-446.1
	IE	47.26	55.58	65.66	68.61	59.28
$n_T = 4$	ΔE_{eq}	1.52	2.13	2.93	3.55	2.53
	Δd_{eq}	0.01	0.02	0.03	0.03	0.02
	$\Delta\omega$	-5.8	-11.7	-31.9	-20.9	-17.6
	IE	1.45	2.26	2.83	3.25	2.45

$\Delta E^{(1)}, n_R = 4$						
n_T		IV.	V.	VI.	VII.	Avg
$n_T = 2$	ΔE_{eq}	38.08	44.22	54.03	61.07	49.35
	Δd_{eq}	0.26	0.31	0.33	0.33	0.31
	$\Delta\omega$	-331.4	-455.1	-636.6	-738.0	-540.3
	IE	60.39	78.48	106.16	121.95	91.75
$n_T = 3$	ΔE_{eq}	1.26	2.43	3.81	5.39	3.22
	Δd_{eq}	0.01	0.02	0.02	0.04	0.02
	$\Delta\omega$	-14.4	-15.0	-31.0	-60.4	-30.2
	IE	1.16	2.31	3.56	5.13	3.04

$\Delta E^{(2)}, n_R = 2$						
n_T		IV.	V.	VI.	VII.	Avg
$n_T = 3$	ΔE_{eq}	18.92	26.34	31.39	33.94	27.65
	Δd_{eq}	0.25	0.27	0.28	0.26	0.26
	$\Delta\omega$	-53.6	-144.1	-233.7	-256.4	-172.0
	IE	32.34	41.13	52.19	56.39	45.51
$n_T = 4$	ΔE_{eq}	18.14	27.34	30.60	33.66	27.43
	Δd_{eq}	0.28	0.34	0.36	0.34	0.33
	$\Delta\omega$	-39.1	-136.4	-141.2	-182.0	-124.6
	IE	32.30	55.27	67.82	68.92	56.08

$\Delta E^{(2)}, n_R = 3$						
n_T		IV.	V.	VI.	VII.	Avg
$n_T = 2$	ΔE_{eq}	12.33	15.46	19.08	20.63	16.88
	Δd_{eq}	0.07	0.08	0.09	0.08	0.08
	$\Delta\omega$	-143.1	-202.4	-259.0	-312.3	-229.2
	IE	12.95	16.79	21.26	22.16	18.29
$n_T = 4$	ΔE_{eq}	4.66	7.24	9.33	10.90	8.03
	Δd_{eq}	0.04	0.08	0.09	0.09	0.08
	$\Delta\omega$	-25.1	-48.3	-56.5	-68.3	-49.6
	IE	4.83	8.69	10.69	11.89	9.03

$\Delta E^{(2)}, n_R = 4$						
n_T		IV.	V.	VI.	VII.	Avg
$n_T = 2$	ΔE_{eq}	19.91	22.19	30.44	33.75	26.57
	Δd_{eq}	0.12	0.12	0.16	0.15	0.14
	$\Delta\omega$	-211.2	-276.1	-418.1	-487.4	-348.2
	IE	22.83	25.10	38.88	42.45	32.31
$n_T = 3$	ΔE_{eq}	-1.30	-3.64	-5.32	-6.49	-4.19
	Δd_{eq}	-0.01	-0.03	-0.03	-0.04	-0.03
	$\Delta\omega$	12.3	12.4	24.0	51.1	24.9
	IE	1.43	3.07	4.39	5.23	3.53

3. Alchemical predictions do not commute

We note the asymmetry in the predictive power of first order based predictions which is due to the lack of commutation: In general $\partial_\lambda E|_{\lambda=0} \neq \partial_\lambda E|_{\lambda=1}$, except if reference and target Hamiltonian happen to differ only by

translation, rotation, or parity (enantiomers, *i.e.* without accounting for parity violation). Within our restricted case of linear interpolations of iso-electronic systems, the perturbing potential does differ only by sign. The integral over its product with the electron density, however, differs in general, *i.e.* $\langle H_A - H_B \rangle_B = \int d\mathbf{r} \rho_B(v_A - v_B) \neq$

$\int d\mathbf{r} \rho_A(v_A - v_B) = -(H_B - H_A)_A$. As such, the error in estimating A based on B will not be the same as the error in estimating B based on A. Results in Table. I suggest that predictions downward the columns in the periodic table are more accurate than upward. For example, predicting HBr using HF as a reference, a better estimate is obtained (error = +25.7 kcal/mol) than for predicting HF using HBr as a reference (error = +61.1 kcal/mol). Correspondingly, predicting HCl using HBr has an error = +5.4 kcal/mol, while the prediction of HBr using HCl has only an error of +3.6 kcal/mol. Similar observations hold for bond lengths, and force constants. The asymmetry is also illustrated in Fig. 2. $\Delta E(d, d_0)$ is not necessarily symmetric with respect to $\lambda = 0.5$ for a given choice of (d, d_0) . Consequently, truncated Taylor series based predictions from either end will not be equally accurate.

4. Chemical accuracy

We have seen that very accurate, yet inexpensive, first order alchemical estimates can be made for vertical alchemical changes between third and fourth row elements according to Eq. (4)—once the density is converged for a given reference molecule. Then, an interesting question is if the alchemical accuracy is on the same order of magnitude as common approximations made when solving Schrödinger’s equation. We have investigated this point for alchemical coupling of HBr and HCl using hybrid and generalized gradient approximated DFT. When using PBE0⁶³ as the method for the reference compound, we find the first order based alchemical predictions according to Eq. (12) to be in better agreement with the PBE0 results for the target compound than true generalized gradient based approximation PBE⁶⁴. Fig. 3 illustrates this point for the covalent binding potentials of HCl and HBr calculated using PBE0, PBE0 based vertical first order alchemical predictions, and PBE. For all interatomic distances in the dissociative tail, the alchemical prediction (squares) is closer to PBE0 (circles) than PBE (diamonds). For the repulsive part of the potential, the alchemical prediction is substantially better than PBE for HBr, and slightly worse than PBE for HCl. For comparison we also included CCSD(T) results. These results amount to numerical evidence that the predictive power of vertical alchemical predictions can exceed the accuracy of common DFT approximations for third or fourth row elements—if a sufficiently accurate electron density is provided for the reference compound.

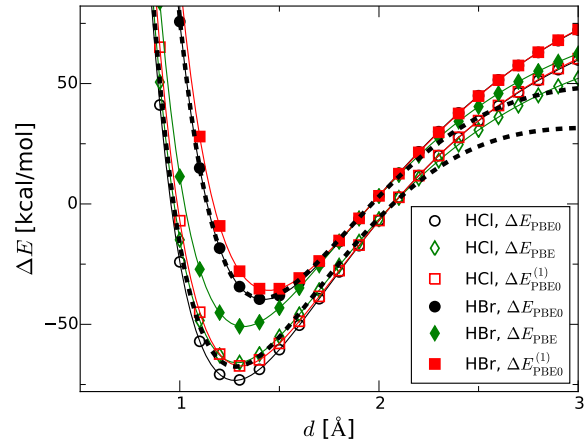


FIG. 3. Alchemical predictions can be more accurate than approximated density functionals. Covalent binding potentials obtained from alchemical PBE0 estimate (red squares) and ordinary PBE (green diamonds) for HBr (full symbols) and HCl (empty symbols). The alchemical estimate corresponds to Eq. (12) using PBE0 density of HBr (HCl) in order to predict HCl (HBr). For comparison, corresponding CCSD(T) results are shown as well (dashed).

B. Vertical iso-valence-electronic changes involving single, double, and triple bonds

1. Predicted potentials

Having discussed covalent bonds involving hydrogen, we now turn to single ($\text{XH}_3\text{-Y}$), double ($\text{XH}_2\text{=Y}$), and triple ($\text{HX}\#\text{Y}$) bonds among p -block elements. Since third row elements can either be alchemically compressed to the corresponding second row ($n = 2$) element in the same column, or expanded to the fourth row ($n = 4$) element, we chose third row ($n = 3$) based reference systems for single, double, and triple bonds, namely SiH_3Cl , SiH_2S , and HSiP . The resulting eight alchemical paths are combinations of changing the Si atom ($\text{Si}\rightarrow\text{C}$, $\text{Si}\rightarrow\text{Ge}$) or its binding partner ($\text{Cl}\rightarrow\text{F}$, $\text{Cl}\rightarrow\text{Br}$, $\text{S}\rightarrow\text{O}$, $\text{S}\rightarrow\text{Se}$, $\text{P}\rightarrow\text{N}$, $\text{P}\rightarrow\text{As}$). In Figs. 4 first and second order alchemical predictions are shown for the bonding potential using vertical transmutations from the three reference molecules.

More specifically, single bonds predictions have been investigated for making predictions using SiH_3Cl as a reference compound for the eight following molecules with 14 valence electrons: CH_3F , CH_3Cl , CH_3Br ($n_X = 2$); SiH_3F , SiH_3Br ($n_X = 3$); and GeH_3F , GeH_3Cl , and GeH_3Br ($n_X = 4$). For double bonds, we have considered predictions for the following eight unsaturated molecules 12 valence electrons and using SiH_2S as a reference compound: CH_2O , CH_2S , CH_2Se ($n_X = 2$); SiH_2O , SiH_2Se ($n_X = 3$); and GeH_2O , GeH_2S , and GeH_2Se ($n_X = 4$). And finally for triple bonds, we have studied the following eight molecules with 10 valence electrons and using HSiP

as a reference compound: HCN, HCP, HCAs ($n_X = 2$); HSiN, HSiAs ($n_X = 3$); and HGeN, HGeP, and HGeAs ($n_X = 4$).

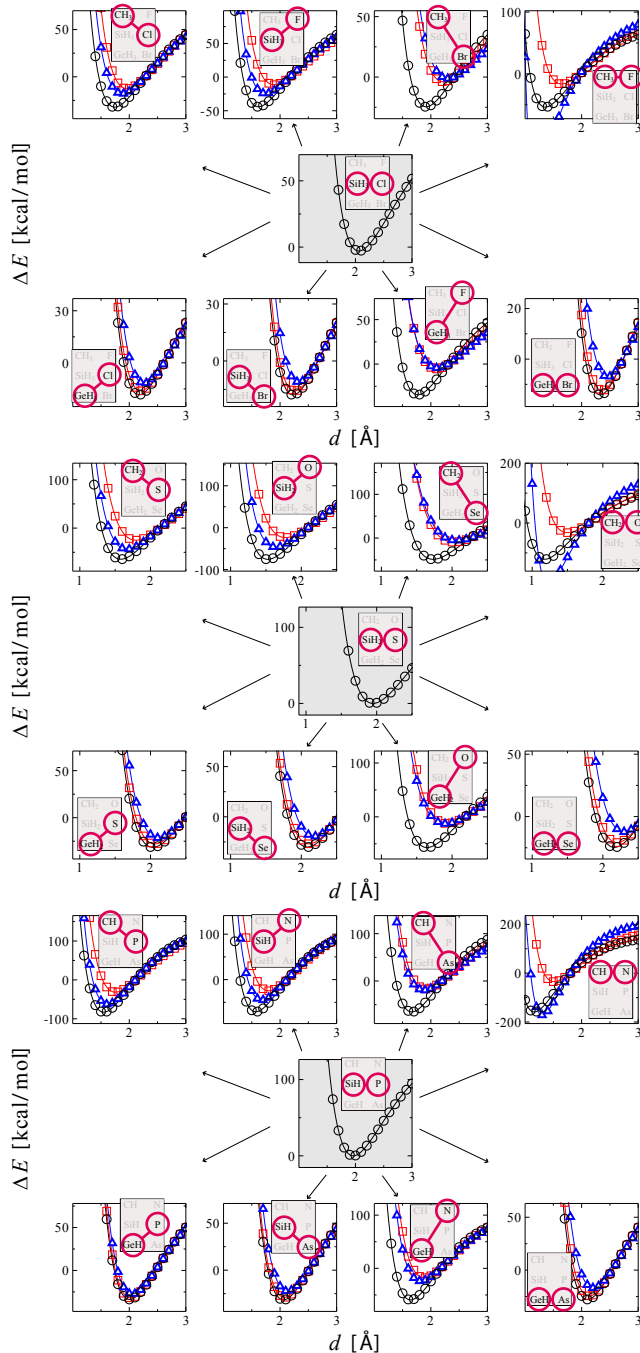


FIG. 4. Alchemical predictions of single (top), double (middle), and triple (bottom) bond potentials. Curves are shown for eight target systems (specified as insets), iso-electronic with reference molecule SiH_3Cl (upper panel), SiH_2S (middle panel), and HSiP (bottom panel) True (black circles), first (red squares) and second (blue triangles) order vertical alchemical predictions of heavy atom bond dissociation curves.

Numerical results in Fig. 4 indicate qualitatively cor-

rect behavior for all predictions. Regarding quantitative performance, the accuracy of the alchemical prediction of $\Delta E(d, d_0)$ exhibits similar behavior as the one discussed above in the case of vertical changes in the hydrogen containing single bond: First order predictions (red) systematically achieve strong predictive power whenever the change involves the coupling of the third row element to a fourth row element. Corresponding second order predictions (blue) deteriorate the accuracy due to inflection points near $\lambda = 0$. If the coupling involves one lighter element from the second row, the prediction is no longer quantitative. However, in these cases, second order predictions provide a slightly superior prediction. If both atoms are simultaneously transmuted to lighter atoms from the second row, *e.g.* $\text{SiH}_3\text{Cl} \rightarrow \text{CH}_3\text{F}$, second order estimates over correct (change of sign) the first order prediction. In the case of one element transmuted upward the column, the other downward, the second order estimate is hardly distinguishable from the first order estimate. We believe that the reason for this is that the coupling to the lighter element on the one site in the molecule yields the concave behavior leading to an improvement in the prediction, while the coupling to the heavier element on the other site in the molecule yields the convex behavior with the inflection point, leading to a deterioration of the prediction. Effectively, these two effects cancel each other and result in the same predictive accuracy as the one obtained for the first order estimate. This rationalization rests on the assumption that the discussion of Fig. 2 can be applied also to linear combination of effects at different transmuted sites.

2. Integrated errors

Above observations are consistent with the quantitative integrated prediction error measures (definitions in Sec. II F) summarized in Table. II. All first order based predictions of target molecules implying a transmutation downward the periodic table (columns 4/3, 3/4, 4/4) exhibit chemical accuracy with at most 1.83 kcal/mol deviation in minimal energy (GeH_2S), at most 0.04 Å deviation in bond length (GeH_2Se), at most -12.82 [cm^{-1}] deviation in wavenumber (SiH_2Se), and at most 1.56 kcal/mol in integrated energy (GeHAs). The best performance is achieved in the case of changing $\text{SiH}_3\text{Cl} \rightarrow \text{GeH}_3\text{Br}$ with energy error $\Delta E = 0.6$ kcal/mol and integrated IE = 0.9 kcal/mol. Corresponding predictions of equilibrium distance deviates 0.03 Å with vibration frequency deviate -1.1 cm^{-1} . First order predictions do not yield quantitative predictive power for changes involving lighter elements (columns 2/3, 3/2, 2/4, 2/2, 4/2). The worst predictions are found for the simultaneous coupling to two lighter elements (column 2/2) with 76.29 kcal/mol, 0.35 Å, -568.76 cm^{-1} , and 41.45 kcal/mol deviation in minimum energy, bond length, harmonic frequency, and integrated energy (HCN).

While for all first order predictions all mutual devi-

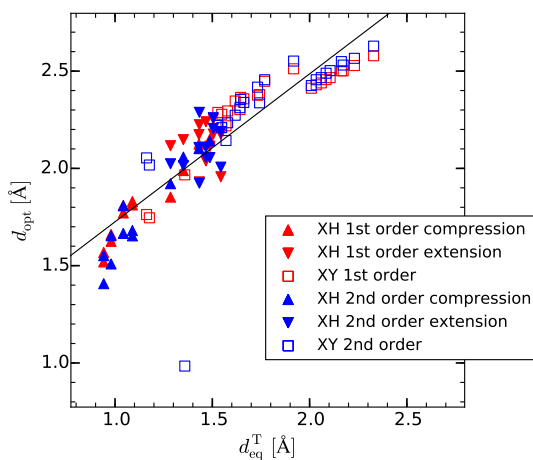


FIG. 5. Scatter plot of optimized reference bond length d_{opt} versus equilibrium bond length of target molecule, denoted by d_{eq}^{T} . Linear regression gives $d_{\text{opt}} = 0.76 d_{\text{eq}} + 0.97 \text{ \AA}$ with MAE=0.11 \AA and RMSE=0.15 \AA . First order (red empty squares) and second order (blue empty triangles) d_{opt} of covalent X-H bond stretching, as well as first order (red filled squares) and second order (blue filled triangles) d_{opt} of X-Y, X=Y, X#Y stretching are shown, where -, =, # stand for single, double, and triple bonds. Some of the alchemical paths are highlighted by black arrows. All numbers are given in Tables I and II in the supplementary material.

ations exhibit the same sign, second order corrections introduce the sign changes in minimum energy and bond length alluded to before, namely both third row elements couple to lighter elements from the second row (column 2/2). Second order predictions for this column are even worse than the corresponding first order predictions. Sec-

D. Non-vertical iso-electronic changes

We are not aware of any mathematical limitation on how to construct alchemical coupling paths under iso-electronic condition. In addition to the investigation of predicted PES of iso-electronic compounds with the same geometry, as discussed in Sec. III A and Sec. III B, we have also investigated if one can use only *one* reference calculation in order to estimate the *entire* PES through “non-vertical” interpolations. In other words, we have also assessed the applicability of the Taylor expansion of Eq. (9) to non-vertical changes for varying geometry and/or atom types and numbers between reference and target molecule.

ond order predictions only improve first order predictions in the case of columns 2/3 and 3/2, alas, not to a degree considered satisfying.

In summary, for changes corresponding to columns 4/3, 3/4, 4/4 first order based estimates yield chemical accuracy. For changes corresponding to columns 2/2, first order based estimates are inaccurate but still better than second order estimates. For changes corresponding to columns 2/4, and 4/2, first order based estimates are similar to second order estimates, yet both are inaccurate. For changes corresponding to columns 2/3 and 3/2, second order based estimates are inaccurate but still better than first order estimates.

C. Empirical d_{opt}

Above observations have been made for optimized d_0 . It should be noted that the choice of d_0 in Eq. (10) is crucial for linearizing the property of interest in alchemical coupling parameter λ , and hence essential for the performance of the perturbation based predictions. We have found that the error minimizing d_{opt} has an approximately linear dependence on the target molecule’s equilibrium bond length d_{eq} , no matter if the reference is the hydrogen containing single bond, or a single, double, or triple bond involving p -block elements from second, third, or fourth row. Furthermore, the linear relationship is preserved, independent of the fact if predictions are made with first or second order estimates. This relationship is shown in Fig. 5. The parameters of a linear regression are specified as well. The outlier in Fig. 5 at target $d_{\text{eq}} \approx 1.35 \text{ \AA}$ and $d_{\text{opt}} \approx 1.0 \text{ \AA}$ is due to the second order prediction of $\text{SiH}_3\text{Cl} \rightarrow \text{CH}_3\text{F}$, i.e. for the above discussed worst case scenario (column 2/2) where a strong overcorrection has been found.

1. Alchemical stretching of H_2^+

We now turn to the case of alchemical stretching of H_2^+ in order to understand the effect of varying geometry on alchemical predictions. Since Hartree-Fock is numerically exact for one-electron systems, we have employed an atomic basis set in an “all-electron” (no PPs) calculation within the following alignment scheme: One proton is centered at $\mathbf{R}_1 = (0, 0, 0)$, the other is aligned along the $+x$ -axis. The reference system corresponds to H_2^+ at its equilibrium bond length. Stretching is accomplished not by pulling the atoms apart but rather by simultaneous annihilation and creation of nuclear charges at $\mathbf{R}_2^{\text{R}} = (d_{\text{eq}}, 0, 0)$ and $\mathbf{R}_2^{\text{T}} = (d, 0, 0)$, respectively. Once the SCF is done for d_{eq} , the entire binding potential can be estimated up to $m = 4$ order, using Eq. (11), by scanning through various d , i.e. setting $d_0 = d_{\text{eq}}$.

Results are shown in Fig. 6(a). Due to the variational

TABLE II. Summary of error measure in Fig. 4 for first (upper table) and second order (lower table) based predictions. The reference molecules are in the left hand column as $H_R = \{\text{SiH}_3\text{Cl}, \text{SiH}_2\text{S}, \text{HSiP}\}$. The primary quantum number of the heavy atoms $X = \{\text{C}, \text{Si}, \text{Ge}\}$ and $Y = \{\text{N}, \text{P}, \text{As}, \text{O}, \text{S}, \text{Se}, \text{F}, \text{Cl}, \text{Br}\}$ in target molecules $\text{XH}_3\text{-Y}$, $\text{XH}_2\text{=Y}$, and $\text{HX}\#\text{Y}$, respectively, are specified using the corresponding principal quantum numbers n_X and n_Y in each column. The right hand column ($n_X = 4/n_Y = 4$), for example, corresponds to predictions of molecules GeH_3Br , GeH_2Se , and HGeAs , respectively. Error measures of each panel are collected in corresponding cell with unit [kcal/mol] for ΔE_{eq} and IE, [\AA] for Δd_{eq} , and $\Delta\omega$ is in [cm^{-1}].

$\Delta E^{(1)}$									
H_R		2/3	3/2	2/4	2/2	4/3	3/4	4/2	4/4
SiH ₃ Cl	ΔE_{eq}	9.04	18.25	10.37	20.37	0.95	0.80	15.83	0.60
	Δd_{eq}	0.22	0.27	0.31	0.29	0.03	0.03	0.33	0.03
	$\Delta\omega$	-91.83	-169.02	-106.27	-237.85	-12.05	-5.02	-148.62	-1.09
	IE	10.14	16.82	12.98	14.85	1.18	0.98	16.74	0.88
SiH ₂ S	ΔE_{eq}	21.69	30.78	22.87	52.34	1.83	1.28	26.77	1.42
	Δd_{eq}	0.21	0.25	0.29	0.32	0.02	0.03	0.28	0.04
	$\Delta\omega$	-191.24	-241.71	-201.69	-436.06	-9.88	-12.82	-218.43	-10.84
	IE	15.16	19.47	14.94	33.25	0.92	0.92	17.18	0.98
SiHP	ΔE_{eq}	31.35	26.34	30.42	76.29	0.79	1.32	23.91	1.28
	Δd_{eq}	0.21	0.23	0.25	0.35	0.01	0.02	0.24	0.03
	$\Delta\omega$	-240.70	-229.35	-250.08	-568.76	-1.77	-9.15	-192.45	-2.34
	IE	22.28	19.42	23.73	41.45	0.93	1.22	18.35	1.56

$\Delta E^{(2)}$									
SiH ₃ Cl	ΔE_{eq}	7.79	11.84	13.29	-103.39	3.00	2.54	17.60	2.68
	Δd_{eq}	0.13	0.13	0.39	-0.18	0.09	0.10	0.34	0.13
	$\Delta\omega$	-91.30	-111.67	-147.58	1912.55	-22.96	-18.27	-176.49	-13.20
	IE	6.48	8.47	16.19	32.26	3.36	3.61	17.63	3.83
SiH ₂ S	ΔE_{eq}	12.46	17.88	28.09	-101.05	5.18	4.59	29.36	5.36
	Δd_{eq}	0.09	0.11	0.33	0.06	0.08	0.09	0.26	0.13
	$\Delta\omega$	-113.32	-128.03	-258.05	1290.29	-36.73	-30.13	-256.16	-27.49
	IE	6.84	9.58	15.34	33.66	2.47	2.75	14.82	2.42
SiHP	ΔE_{eq}	12.04	14.92	30.85	-50.92	3.05	4.22	21.95	4.93
	Δd_{eq}	0.07	0.11	0.22	0.14	0.04	0.07	0.18	0.10
	$\Delta\omega$	-94.83	-118.62	-256.64	747.69	-11.84	-29.35	-182.63	-22.36
	IE	8.56	9.45	21.74	28.53	2.96	4.58	14.80	5.71

principle for linearly coupled alchemical Hamiltonians,¹² $\Delta E^{(1)} > \Delta E$ for all interatomic distances. Inclusion of second order term improves upon the first order prediction, yielding a reasonable binding potential. However, when including third and fourth order the performance deteriorates again with oscillating behaviour for varying order (Fig. 6(a) and inset of (b)), as $\Delta E^{(3)}$ overshoot and $\Delta E^{(4)}$ over corrects. Overall $\Delta E^{(2)}$ gives the best prediction.

To explain the oscillating behaviour in Taylor expansion order, we investigate in more detail how the system responds to alchemical perturbation. When λ increases gradually from 0 to 1, the nuclear charge decreases from 1 to 0 at \mathbf{R}_2^R , while increasing from 0 to 1 at \mathbf{R}_2^T . Using the alchemical derivatives at $\lambda = 0$, truncated Taylor series based estimates are plotted along the true energy in Fig. 6(b) as a function of λ at $d = 3 \text{ \AA}$. $\Delta E^{(1)}$, $\Delta E^{(2)}$, $\Delta E^{(3)}$, and $\Delta E^{(4)}$ are linear, quadratic, third order, and fourth order polynomials, respectively. Clearly, the truncated Taylor series will fail to converge to ΔE at $\lambda = 1$ due to a sharp change of ΔE at $\lambda \approx 0.9$. This implies a strong nonlinear electronic response occurring late in the alchemical coupling regime, resulting in the oscillat-

ing behaviour of the predicted PES in Figs. 6(a) and (b). Note that while the sign of error alternates, the magnitude of error also increases as one increases the order. Similar behaviour can be observed for other values of d .

The energy gain starting at $\lambda \approx 0.9$ is due to a rapid rearrangement of electron density for $\lambda > 0.9$. This is illustrated in Fig. 6(c) where the integrated electron density $P_\lambda(x)$ is plotted as a function of both λ and x at $d = 3 \text{ \AA}$. Cohen and Mori-Sánchez already pointed out for H_2^+ the dramatic changes in electronic structure for infinitesimally small changes in nuclear charges at infinite distance.⁶⁵ One would expect this effect to intensify as more basis functions are taken into account. This behaviour can be seen in Fig. 6(c). The locations of the proton at origin \mathbf{R}_1 , as well as the location of the annihilated proton at \mathbf{R}_2^R , and created proton at \mathbf{R}_2^T , are indicated by red lines.

Further analysis shows that for $\lambda > 0.5$, both ground and first excited state orbitals are localized: The electronic ground state is localized at \mathbf{R}_1 while the first excited state is localized at \mathbf{R}_2^T . At $\lambda \approx 0.9$, the two eigenvalues become degenerate, resulting in a rapid change of the ground state density in order to meet the non polar

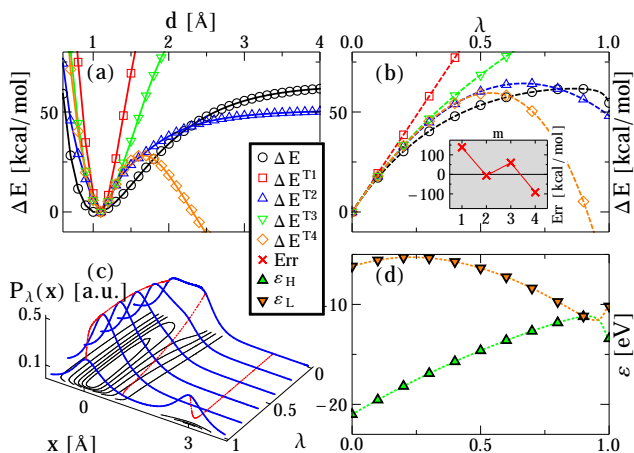


FIG. 6. m^{th} order truncated Taylor series of H_2^+ are denoted by $\Delta E^{(m)}$ in (a) as a function of d at $\lambda = 1$ and in (b) as a function of λ at $d = 3$ Å. Inset shows the error of $\Delta E^{(m)}$ at $\lambda = 1$ (c) Integrated density $P_\lambda(x) = \int dydz \rho_\lambda(\mathbf{r})$ where $\mathbf{r} = (x, y, z)$, is presented as a function of both λ and x at $d = 3$ Å where the integrated density values at nuclei locations highlighted by red lines at $x = 0$ Å, $x = 1.1$ Å, and $x = 3$ Å, while contour lines are drawn at the bottom. (d) HOMO/LUMO levels, denoted by ε_H and ε_L respectively, are plotted as a function of λ at $d = 3$ Å.

symmetry requirement of H_2^+ , by taking a linear combination of both ground and first excited state. Note that there is no orbital node at midpoint, indicating a true ground state for a dissociated H_2^+ molecule. The degeneracy occurs for the system with fractional nuclear charges at $\lambda \approx 0.9$. The dramatic change in density stabilizes the system in λ , giving rise to the sharp decrease in energy in Fig. 6(b), as λ increases from 0.8 to 1. Perturbation theory for degenerate cases might be necessary to properly account for this case. The degeneracy of the ground state and first excited state is shown for the eigenvalue crossing in Fig. 6(d): The eigenvalue of the (highest) occupied molecular orbital (HOMO) and lowest unoccupied molecular orbital (LUMO) are plotted as a function of λ . The degeneracy breaks when ground state and first excited state switch order, which results in a delocalized ground state. By contrast, note that the eigenvalues will not cross each other if the stretching is carried out by moving \mathbf{R}_2^R in real space.

Crossing of eigenvalue surfaces limits the radius of convergence of alchemical Taylor expansion series within electronic ground-state theories. As a result, the Taylor expansion for this system is not convergent at $\lambda = 1$, similar to well known cases in Møller-Ploeset theory.^{66–68} For asymmetric alchemical interpolations, as exemplified for the following examples in this study, as well as in previous studies,^{11,17,20,32} the energy is typically smooth in all λ values, and derivative based expansions are expected to converge.

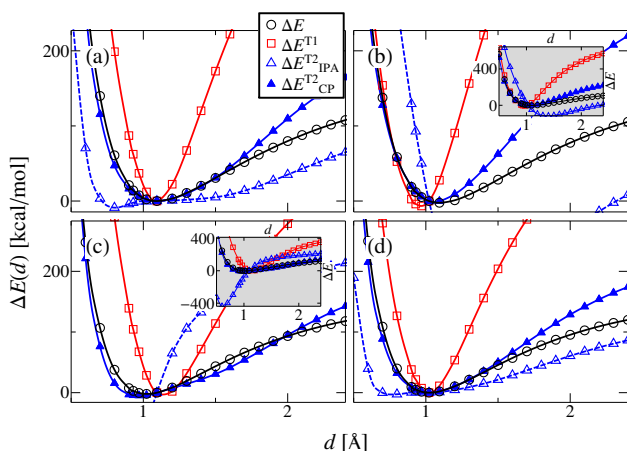


FIG. 7. Energy difference ΔE , first order truncated Taylor series $\Delta E^{(1)}$, second order truncated Taylor series calculated by coupled perturbed $\Delta E_{\text{CP}}^{(2)}$, and second order truncated Taylor series calculated by independent particle approximation $\Delta E_{\text{IPA}}^{(2)}$ are plotted as black circles, red squares, blue open triangles, and blue filled triangles respectively. Coupling Hamiltonians are arranged as follow: (a) $\text{CH}_4 \rightarrow \text{CH}_4$, (b) $\text{NH}_3 \rightarrow \text{CH}_4$, (c) $\text{CH}_4 \rightarrow \text{NH}_3$, and (d) $\text{NH}_3 \rightarrow \text{NH}_3$. Insets of (b) and (c) show the zoom-out energy scale for overall landscape.

2. Non-vertical iso-electronic changes in ten electron systems

In the final section of this paper, we consider alchemical non-vertical changes of molecules with ten electrons. More specifically, we present numerical results of non-vertical iso-electronic changes involving bond stretching in second row systems $\{\text{CH}_4, \text{NH}_3, \text{H}_2\text{O}, \text{HF}\}$, using all electron DFT. The H_2^+ example has indicated that non-vertical changes can profit from second order estimates. Since exact analytical expressions are not available for systems with so many electrons, and since no PPs are involved, we have relied on approximative second order expressions IPA and CP, rather than on finite difference expressions (see Methods section above).

3. Predicted potentials

Fig. 7 illustrates the prediction of R-H covalent bond potentials for CH_4 and NH_3 , predicted from alchemical derivatives using the electronic structure obtained by a single SCF. As a reference system we used once the relaxed CH_4 system (panels (a), (c)), and once the relaxed NH_3 (panels (b), (d)) geometry. For the chemical composition of H_R being the same as H_T and only the bond being stretched (Fig. 7(a), (d)), the first order estimate constitutes an upper bound, *i.e.* it always overshoots due to the concave behaviour of ΔE as a function of λ , also on display in Fig. 6(b). When also changing the chemical compositions from CH_4 and NH_3 or vice versa, the

TABLE III. Prediction errors using first and second order based alchemical estimates for non-vertical changes in ten electron systems. Deviation of predicted energy minimum from actual ΔE_{eq} [kcal/mol], corresponding bond length deviation Δd_{eq} [Å], and vibration frequency $\Delta\omega_{\text{eq}}$. Numerical results from first order $\Delta E^{(1)}$, second order with independent particle approximation $\Delta E_{\text{IPA}}^{(2)}$, and second order with coupled perturbed $\Delta E_{\text{CP}}^{(2)}$ truncated Taylor series are presented. Average is calculated for each row in Avg column.

$\Delta E^{(1)}$:						
H_{R}		CH ₄	NH ₃	H ₂ O	HF	Avg
CH ₄	ΔE_{eq}	-0.22	-2.30	-9.63	-21.99	-8.54
	Δd_{eq}	-0.01	0.12	0.22	0.30	0.15
	$\Delta\omega$	6061.	3545.	2641.	1874.	3530.
NH ₃	ΔE_{eq}	-4.33	-0.04	-4.34	-14.01	-5.68
	Δd_{eq}	-0.13	0.002	0.10	0.19	0.04
	$\Delta\omega$	4218.	4268.	4622.	2449.	3889.
H ₂ O	ΔE_{eq}	-32.78	-5.97	-0.0000	-4.88	-10.91
	Δd_{eq}	-0.27	-0.11	0.0005	0.09	-0.07
	$\Delta\omega$	4360.	3933.	3886.	2568.	3687.
HF	ΔE_{eq}	-120.8	-38.63	-7.95	0.0003	-41.85
	Δd_{eq}	-0.44	-0.25	-0.10	-0.0008	-0.20
	$\Delta\omega$	5772.	4047.	3982.	3560.	4340.
$\Delta E_{\text{IPA}}^{(2)}$:						
CH ₄	ΔE_{eq}	-8.99	-437.5	-935.2	-1356.	-684.4
	Δd_{eq}	-0.31	-0.41	-0.40	-0.39	-0.38
	$\Delta\omega$	2207.	9625.	12610.	14600.	9761.
NH ₃	ΔE_{eq}	-113.4	-4.10	-673.2	-1394.	-546.1
	Δd_{eq}	0.29	-0.27	-0.45	-0.43	-0.21
	$\Delta\omega$	470.9	1471.	11200.	12660.	6452.
H ₂ O	ΔE_{eq}	-198.7	-90.18	-0.007	-809.4	-274.6
	Δd_{eq}	0.16	0.21	0.007	-0.43	-0.01
	$\Delta\omega$	2949.	1124.	-1484.	9157.	2937.
HF	ΔE_{eq}	-212.6	-140.4	-64.95	0.002	-104.5
	Δd_{eq}	0.05	0.11	0.15	-0.001	0.08
	$\Delta\omega$	6035.	4110.	1975.	-1177.	2736.
$\Delta E_{\text{CP}}^{(2)}$:						
CH ₄	ΔE_{eq}	-0.39	-2.74	-19.70	-41.12	-15.99
	Δd_{eq}	-0.02	-0.07	-0.10	-0.10	-0.07
	$\Delta\omega$	1663.	-495.7	2116.	3584.	1717.
NH ₃	ΔE_{eq}	0.90	-0.04	-1.84	-15.17	-4.04
	Δd_{eq}	-0.04	0.007	-0.06	-0.10	-0.05
	$\Delta\omega$	2133.	140.4	-1480.	1690.	620.9
H ₂ O	ΔE_{eq}	5.78	0.77	0.0000	-1.51	1.26
	Δd_{eq}	-0.08	-0.02	0.002	-0.04	-0.03
	$\Delta\omega$	2207.	-75.3	-194.2	-345.3	398.0
HF	ΔE_{eq}	13.12	4.25	0.65	0.001	4.50
	Δd_{eq}	-0.14	-0.07	-0.02	-0.0006	-0.06
	$\Delta\omega$	3501.	2272.	1074.	-247.5	1650.

first order estimate does not even capture the changes in equilibrium bond length (Fig. 7(b) and (c)).

$\Delta E_{\text{IPA}}^{(2)}$ yields a saddle point in Fig. 7(a) and (d), instead of a minimum at optimized geometry. When the chemical compositions of H_{R} and H_{T} are different, $\Delta E_{\text{IPA}}^{(2)}$ results in in dramatic errors (worse than first order estimates), as shown in the energy zoom out in the

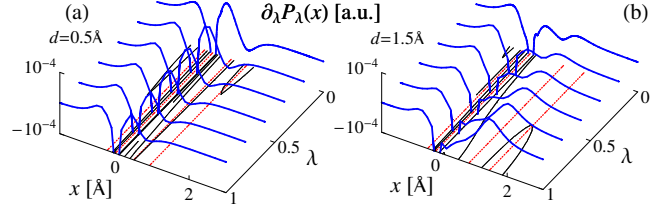


FIG. 8. $\partial_{\lambda} P_{\lambda}(x)$ is calculated by finite difference $\partial_{\lambda} P_{\lambda}(x) \approx \frac{P_{\Delta\lambda}(x) - P_{\lambda=0}(x)}{\Delta\lambda}$. $\partial_{\lambda} P_{\lambda}(x)$, of HF \rightarrow H₂O at (a) $d = 0.5$ Å for compression and at (b) $d = 1.5$ Å for extension are plotted as a function of x and λ . Nuclear positions are highlighted by red dashed lines, with F \rightarrow O at $x = 0$ Å, H \rightarrow void at $x = 0.93$ Å, two void \rightarrow H at $x = -0.22$ Å and $x = d$, where void denotes the nuclei with zero charge.

insets of Fig. 7(b) and (c). The poor predictive power of IPA has also recently been pointed out by Pulay and co-workers⁶⁹. By contrast, $\Delta E_{\text{CP}}^{(2)}$ yields a very reasonable binding potential, albeit still far from being chemically accurate. The superior performance of $\Delta E_{\text{CP}}^{(2)}$, with respect to $\Delta E_{\text{IPA}}^{(2)}$, indicates that the contributions of Coulomb and xc energy due to density response are crucial. In other words, matrix elements $\mathbf{J}_{ia,jb}$ and $\mathbf{X}_{ia,jb}$ in Eq. (8) should not be neglected for non-vertical alchemical perturbations.

Different predictive accuracy is found for compressing bonds $d < d_{\text{eq}}$ versus stretching bonds $d > d_{\text{eq}}$. $\Delta E_{\text{CP}}^{(2)}$ performs better in the region $0.5 \text{ Å} \leq d \leq 1.5 \text{ Å}$. Similar behaviour is also observed for other alchemical paths of compressing vs stretching bond. Also in this case, the aforementioned non-commutative asymmetric behavior of the predictions is observed. Namely, the $\Delta E_{\text{CP}}^{(2)}$ based prediction for CH₄ \rightarrow NH₃ in Fig. 7(c) is more accurate than for NH₃ \rightarrow CH₄ in Fig. 7(b). Note that abrupt changes in electronic structure, as observed for H₂⁺ in Sec. III D 1, are not present when coupling these systems.^{70,71} Since the accuracy of the second order estimate is determined by how linearly the electron density rearranges as a function of λ , one expects a near-constant $\partial_{\lambda}\rho$ for negligible higher order contributions. This is confirmed through inspection of the integrated density response of the alchemical path HF \rightarrow H₂O in Fig. 8. $\partial_{\lambda} P_{\lambda}(x)$ varies less when λ changes from zero to one for $d = 0.5$ Å Fig. 8(a), when compared with $d = 1.5$ Å Fig. 8(b). A near constant $\partial_{\lambda} P_{\lambda}(x)$ at $d = 0.5$ Å results in improved predictive accuracy.

4. Integrated errors

Table. III summarizes the results for all 4×4 combinations of $H_{\text{R}} \rightarrow H_{\text{T}}$, where mutual predictions of covalent bond potentials in H_{T} : {CH₄, NH₃, H₂O, HF} are obtained based on only the single point wavefunctions obtained for the relaxed geometry of H_{R} : {CH₄,

NH_3 , H_2O , HF }, respectively. This coupling matrix in chemical space (Table. III) is not symmetric (due to the non-commutative properties discussed above). Off-diagonal elements correspond to coupling paths involving changes in chemical composition *and* geometry. Diagonal elements correspond to coupling paths that involve only changes in geometry, i.e. for the same stoichiometry. Note that all error measures have been obtained via cubic spline fits. Therefore, also the predicted ΔE and the location of the energy minimum can be slightly non-zero even for the diagonal elements. These values should be considered noise: For the diagonal elements only the harmonic frequencies are meaningful.

Table. III confirms the trends observed above for first and second order. In general, best predictive power is found when the chemical composition of H_R is the same as H_T (diagonal elements). When the chemical composition of H_T differs from H_R the predictive accuracy deteriorates. This is not surprising and due to the perturbing Coulomb potential being placed on the heavy atom in order to mutate it, e.g. from carbon to fluorine. Because of the strong accumulation of electron density (cusps) at the heavy atom’s site (6 to 7 electrons for carbon to fluorine, respectively), this perturbation is quite severe. In the case of the diagonal element, by contrast, only the hydrogen atom is being annihilated and created, implying that the perturbing potential acts on the hydrogen atom’s electronic density which is built up by only 1 electron. This implies a less severe perturbation, and therefore worse predictive power can be expected for off-diagonal elements.

The crucial importance of Coulomb and xc energy contribution to density response for second order alchemical perturbation is also confirmed for the other cases in Table. III. These results clearly underscore the observation that IPA is a (very) poor approximation when it comes to estimate alchemical changes, yielding even worse predictions than the first order estimates. Interestingly enough, the first order estimate is even competitive in comparison to the second order CP predictions. For example, using CH_4 as a reference compound the first order prediction deviates on average by -8.54 kcal/mol in the energy, while $\Delta E_{\text{CP}}^{(2)}$ deviates -15.99 kcal/mol. However, as the reference compound moves to the right hand side of the periodic table, the second order CP based estimate becomes more accurate than the first order based estimate.

An additional aspect can be confirmed from inspection of Table. III: The larger the perturbing potential, the worse the predictive accuracy of derivative based estimate. More specifically, the larger the integrated norm of the difference between reference and target potential in the electronic Hamiltonian, the worse the predictive power. For example, using CH_4 as a reference compound, the prediction will be increasingly worse in the order of the respective predictions for NH_3 , H_2O , and HF . Conversely, using HF as a reference compound, the prediction will be increasingly worse in the order of the respective

predictions for H_2O , NH_3 , and CH_4 . Note that this is true for all first as well as second order estimates.

IV. CONCLUSIONS

The performance of truncated Taylor series for predicting alchemical vertical changes in covalent bonding has been investigated in iso-electronic chemical spaces spanned by the external potentials of small molecules. For vertical linear transmmutations (same geometry, same number of atoms, differing nuclear charges) our results suggest that chemical accuracy is possible when interpolating molecules containing p -block atoms from the third and fourth row using first order (Hellmann-Feynman theory) based predictions. Since first order estimates are analytical, this finding implies that one can scan potential energy surfaces of very many molecules with unprecedented accuracy and speed as long as their stoichiometries are restricted to third and fourth row main group chemistries. First order based predictions of chemistries involving second row elements are only correct to a degree considered qualitative.

Overall, we have found second order estimates to not provide sufficient improvement with respect to first order predictions (often even worse results) to warrant the investment in the additional overhead incurred. First order estimates are more accurate not because higher order terms are negligible, but rather due to the fact that (a) changes in relative energies (bonding) are already near-linear (by optimizing the reference geometry) with respect to alchemical coupling (effectively canceling higher order terms), and (b) inflection points can occur which lead to worse predictions for second order estimates. For the interpolation of the pseudopotentials used in this study, inflection points near $\lambda = 0$ are always observed when a lighter main group element is coupled to a heavier one. The absence of inflection points near $\lambda = 1$ improves the predictive power of the second order correction: As such, the asymmetry of $\Delta E(d, d_0)$ with respect to $\lambda = 0.5$ results in asymmetric predictive performance.

The choice of the reference geometry has a dramatic impact on the predictive power of the alchemical estimates. For covalent bond potentials, a linear relationship has been identified, ($d_{\text{opt}} \approx 0.76 d_{\text{eq}}^T + 0.97 \text{ \AA}$), that can be used to predict optimal d_0 requiring only rough estimates of the equilibrium bond-length in the target molecule (which can easily be obtained using universal force-fields or semi-empirical quantum chemistry methods).

We have found oscillating behaviour in the predictions of truncated Taylor series when varying the order in the non-vertical alchemical stretching of H_2^+ . The crossing of eigenvalue surfaces is due to the electron density’s necessity to be symmetric at $\lambda = 0$ and $\lambda = 1$. This leads to a diverging series Taylor series, yet the second order correction could still provide fair predictions. The behavior of first and second order truncated alchemical Tay-

lor series expansions in non-vertical transmutations in chemical space has also been analyzed for molecules with ten electrons. Numerical evidence of the superior performance of $\Delta E_{\text{CP}}^{(2)}$ over $\Delta E_{\text{IPA}}^{(2)}$ suggests that the response of Coulomb and xc energy to alchemical perturbation is crucial.

In summary, our findings indicate that a careful choice of alchemical interpolation paths enables alchemical derivatives to achieve predictive power with chemical accuracy for covalent bond potentials. Future work will deal with angles and torsions in larger molecules, as well as with solid metals and ionic crystals.

V. ACKNOWLEDGEMENTS

We would like to thank K. Morokuma, E. Tapavicza, Q. Cui, A. Alavi, P. Ayers and P. Geerlings for discussions. OAvL acknowledges funding from the Swiss National Science foundation (No. PP00P2_138932). SF acknowledges the Research Foundation Flanders (FWO) for financial support. Some calculations were performed at sciCORE (<http://scicore.unibas.ch/>) scientific computing core facility at University of Basel.

* anatole.vonlilienfeld@unibas.ch

- ¹ E. Schrödinger, "An undulatory theory of the mechanics of atoms and molecules," *Phys. Rev.*, vol. 28, p. 1049, 1926.
- ² P. A. M. Dirac, "Quantum mechanics of many-electron systems," *Proc. Math. Phys. Eng. Sci.*, vol. 123, p. 714, 1929.
- ³ J. Harris, "Simplified method for calculating the energy of weakly interacting fragments," *Phys. Rev. B*, vol. 31, p. 1770, 1985.
- ⁴ J. Harris, "Tight-binding models and density-functional theory," *Phys. Rev. B*, vol. 39, p. 12520, 1989.
- ⁵ D. Benoit, D. Sebastiani, and M. Parrinello, "Accurate total energies without self-consistency," *Phys. Rev. Lett.*, vol. 87, p. 226401, 2001.
- ⁶ S. R. Marder, D. N. Beratan, and L. T. Ceng, "Approaches for optimizing the first electronic hyperpolarizability of conjugated organic molecules," *Science*, vol. 252, p. 103, 1991.
- ⁷ A. Franceschetti and A. Zunger, "The inverse band-structure problem of finding an atomic configuration with given electronic properties," *Nature*, vol. 402, p. 60, 1999.
- ⁸ G. H. Jóhannesson, T. Bliigaard, A. V. Ruban, H. L. Skriver, K. W. Jacobsen, and J. K. Nørskov, "Combined electronic structure and evolutionary search approach to materials design," *Phys. Rev. Lett.*, vol. 88, p. 255506, 2002.
- ⁹ O. A. von Lilienfeld, *Towards the Computational Design of Compounds from First Principles*, vol. IX of *Mathematical Physics Studies*. Springer, 2014. Editors: V. Bach and L. Delle Site.
- ¹⁰ T. F. T. Cerqueira, R. Sarmiento-Prez, M. Amsler, F. Nogueira, S. Botti, and M. A. L. Marques, "Materials design on-the-fly," *J. Chem. Theory Comput.*, vol. 11, no. 8, pp. 3955–3960, 2015.
- ¹¹ O. A. von Lilienfeld and M. E. Tuckerman, "Molecular grand-canonical ensemble density functional theory and exploration of chemical space," *J. Chem. Phys.*, vol. 125, p. 154104, 2006.
- ¹² O. A. von Lilienfeld, "First principles view on chemical compound space: Gaining rigorous atomistic control of molecular properties," *Int. J. Quantum Chem.*, vol. 113, p. 1676, 2013.
- ¹³ C. Kuhn and D. N. Beratan, "Inverse strategies for molecular design," *J. Phys. Chem.*, vol. 100, p. 10596, 1996.
- ¹⁴ M. E. M. Noble, J. A. Endicott, and L. N. Johnson, "Protein kinase inhibitors: Insights into drug design from structure," *Science*, vol. 303, p. 1800, 2004.
- ¹⁵ S. Keinan, X. Hu, D. Beratan, and W. Yang, "Designing molecules with optimal properties using the linear combination of atomic potentials approach in an AM1 semiempirical framework," *J. Phys. Chem.*, vol. 111, p. 176, 2007.
- ¹⁶ R. Car and M. Parrinello, "Unified approach for molecular dynamics and density functional theory," *Phys. Rev. Lett.*, vol. 55, p. 2471, 1985.
- ¹⁷ O. A. von Lilienfeld, R. D. Lins, and U. Rothlisberger, "Variational particle number approach for rational compound design," *Phys. Rev. Lett.*, vol. 95, p. 153002, 2005.
- ¹⁸ M. Wang, X. Hu, D. N. Beratan, and W. Yang, "Designing molecules by optimizing potentials," *J. Am. Chem. Soc.*, vol. 128, p. 3228, 2006.
- ¹⁹ V. Marcon, O. A. von Lilienfeld, and D. Andrienko, "Tuning electronic eigenvalues of benzene via doping," *J. Chem. Phys.*, vol. 127, p. 064305, 2007.
- ²⁰ O. A. von Lilienfeld, "Accurate *ab initio* energy gradients in chemical compound space," *J. Chem. Phys.*, vol. 131, p. 164102, 2009.
- ²¹ D. Sheppard, G. Henkelman, and A. von Lilienfeld, "Alchemical derivatives of reaction energetics," *J. Chem. Phys.*, vol. 133, p. 084104, 2010.
- ²² T. Weymuth and M. Reiher, "Inverse quantum chemistry: Concepts and strategies for rational compound design," *Int. J. Quantum Chem.*, vol. 114, p. 823, 2014.
- ²³ B. Widom, "Some topics in the theory of fluids," *J. Chem. Phys.*, vol. 39, no. 11, pp. 2808 – 2812, 1963.
- ²⁴ M. D. Macedonia and E. J. Maginn, "A biased grand canonical monte carlo method for simulating adsorption using all-atom and branched united atom models," *Mol. Phys.*, vol. 96, p. 1375, 1999.
- ²⁵ M. D. Macedonia and E. J. Maginn, "Pure and binary component sorption equilibria of light hydrocarbons in the zeolite silicalite from grand canonical monte carlo simulations," *Fluid Phase Equilibria*, vol. 158-160, p. 19, 1999.
- ²⁶ W. L. Jorgensen and C. Ravimohan, "Monte Carlo simulation of differences in free energies of hydration," *J. Chem. Phys.*, vol. 83, p. 3050, 1985.
- ²⁷ W. G. van Gunsteren and H. J. C. Berendsen, "Thermodynamic cycle integration by computer simulation as a tool for obtaining free energy differences in molecular chemistry," *J. Comput. Aided Mol. Des.*, vol. 1, p. 171, 1987.
- ²⁸ T. Straatsma and J. A. McCammon, "Computational alchemy," *Annu. Rev. Phys. Chem.*, vol. 43, p. 407, 1992.

- ²⁹ C. Oostenbrink and W. F. van Gunsteren, "Free energies of ligand binding for structurally diverse compounds," *Proc. Natl. Acad. Sci. USA*, vol. 102, p. 6750, 2005.
- ³⁰ S. Riniker, C. D. Christ, H. S. Hansen, P. H. Hünenberger, C. Oostenbrink, D. Steiner, and W. F. van Gunsteren, "Calculation of relative free energies for ligand-protein binding, solvation, and conformational transitions using the GROMOS software," *J. Phys. Chem. B*, vol. 115, p. 13570, 2011.
- ³¹ J. E. Bright Wilson, "Four-dimensional electron density function," *J. Phys. Chem.*, vol. 36, p. 2232, 1962.
- ³² K. Y. S. Chang and O. A. von Lilienfeld, "Quantum mechanical treatment of variable molecular composition: From 'alchemical' changes of state function to rational compound design," *CHIMIA*, vol. 68, p. 602, 2014.
- ³³ R. P. Feynman, "Forces in molecules," *Phys. Rev.*, vol. 56, p. 340, 1939.
- ³⁴ O. A. von Lilienfeld and M. E. Tuckerman, "Alchemical variations of intermolecular energies according to molecular grand-canonical ensemble density functional theory," *J. Chem. Theory Comput.*, vol. 3, p. 1083, 2007.
- ³⁵ R. Balawender, M. A. Welearegay, M. Lesiuk, F. De Proft, and P. Geerlings, "Exploring chemical space with the alchemical derivatives," *J. Chem. Theory Comput.*, vol. 9, p. 5327, 2013.
- ³⁶ E. K. U. Gross and W. Kohn, "Local density-functional theory of frequency dependent linear response," *Phys. Rev. Lett.*, vol. 55, p. 2850, 1986.
- ³⁷ W. Yang, A. J. Cohen, F. De Proft, and P. Geerlings, "Analytical evaluation of Fukui function and real space linear response function," *J. Chem. Phys.*, vol. 136, p. 144110, 2012.
- ³⁸ N. Sablon, F. De Proft, P. W. Ayers, and P. Geerlings, "Computing second-order functional derivatives with respect to the external potential," *J. Chem. Theory Comput.*, vol. 6, p. 3671, 2010.
- ³⁹ R. G. Parr and W. Yang, *Density-Functional Theory of Atoms and Molecules*. Oxford University Press, USA, 1994.
- ⁴⁰ A. Putrino, D. Sebastiani, and M. Parrinello, "Generalized variational density functional perturbation theory," *J. Chem. Phys.*, vol. 113, p. 7102, 2000.
- ⁴¹ H. F. Wilson, F. Gygi, and G. Galli, "Efficient iterative method for calculations of dielectric matrices," *Phys. Rev. B*, vol. 78, p. 113303, 2008.
- ⁴² N. Sablon, F. De Proft, and P. Geerlings, "The linear response kernel: Inductive and resonance effects quantified," *J. Phys. Chem. Lett.*, vol. 1, p. 1227, 2010.
- ⁴³ S. Fias, Z. Boisdenghen, T. Stuyver, M. Audiffred, G. Merino, P. Geerlings, and F. De Proft, "Analysis of aromaticity in planar metal systems using the linear response kernel," *J. Phys. Chem. A*, vol. 117, p. 3556, 2013.
- ⁴⁴ P. Geerlings, S. Fias, Z. Boisdenghen, and F. De Proft, "Conceptual DFT: Chemistry from the linear response function," *Chem. Soc. Rev.*, vol. 43, p. 4989, 2014.
- ⁴⁵ S. Baroni, S. de Gironcoli, A. Dal Corso, and P. Giannozzi, "Phonons and related crystal properties from density-functional perturbation theory," *Rev. Mod. Phys.*, vol. 73, pp. 515–562, 2001.
- ⁴⁶ S. L. Adler, "Quantum theory of the dielectric constant in real solids," *Phys. Rev.*, vol. 126, no. 2, p. 413, 1962.
- ⁴⁷ N. Wiser, "Dielectric constant with local field effects included," *Phys. Rev.*, vol. 129, no. 1, p. 62, 1963.
- ⁴⁸ C. Møller and M. S. Plesset, "Note on an approximation treatment for many-electron systems," *Phys. Rev.*, vol. 46, p. 618, 1934.
- ⁴⁹ D. Cremer, "Møller-Plesset perturbation theory: From small molecule methods to methods for thousands of atoms," *Adv. Rev.*, vol. 1, p. 509, 2012.
- ⁵⁰ L. Kleinman and D. M. Bylander, "Efficient form for model pseudopotentials," *Phys. Rev. Lett.*, vol. 48, p. 1425, 1982.
- ⁵¹ O. A. von Lilienfeld, I. Tavernelli, U. Rothlisberger, and D. Sebastiani, "Optimization of effective atom centered potentials for London dispersion forces in density functional theory," *Phys. Rev. Lett.*, vol. 93, p. 153004, 2004.
- ⁵² O. A. von Lilienfeld and P. A. Schultz, "Structure and band gaps of Ga-(V) semiconductors: The challenge of Ga pseudopotentials," *Phys. Rev. B*, vol. 77, p. 115202, 2008.
- ⁵³ O. A. v. Lilienfeld, "Force correcting atom centred potentials for generalised gradient approximated density functional theory: Approaching hybrid functional accuracy for geometries and harmonic frequencies in small chlorofluorocarbons," *Molecular Physics*, vol. 111, no. 14-15, pp. 2147–2153, 2013.
- ⁵⁴ J. P. Perdew, K. Burke, and M. Ernzerhof, "Generalized gradient approximation made simple," *Phys. Rev. Lett.*, vol. 77, p. 3865, 1996.
- ⁵⁵ W. Andreoni and A. Curioni, "New advances in chemistry and materials science with CPMD and parallel computing," *Parallel Computing*, vol. 26, pp. 819–842, 2000.
- ⁵⁶ S. Goedecker, M. Teter, and J. Hutter, "Separable dual-space gaussian pseudopotentials," *Phys. Rev. B*, vol. 54, p. 1703, 1996.
- ⁵⁷ C. Hartwigsen, S. Goedecker, and J. Hutter, "Relativistic separable dual-space gaussian pseudopotentials from H to Rn," *Phys. Rev. B*, vol. 58, p. 3641, 1998.
- ⁵⁸ M. Krack, "Pseudopotentials for H to Kr optimized for gradient-corrected exchange-correlation functionals," *Theor. Chim. Acta*, vol. 114, p. 145, 2005.
- ⁵⁹ M. J. Frisch, G. W. Trucks, H. B. Schlegel, G. E. Scuseria, M. A. Robb, J. R. Cheeseman, G. Scalmani, V. Barone, B. Mennucci, G. A. Petersson, H. Nakatsuji, M. Caricato, X. Li, H. P. Hratchian, A. F. Izmaylov, J. Bloino, G. Zheng, J. L. Sonnenberg, M. Hada, M. Ehara, K. Toyota, R. Fukuda, J. Hasegawa, M. Ishida, T. Nakajima, Y. Honda, O. Kitao, H. Nakai, T. Vreven, J. A. Montgomery, Jr., J. E. Peralta, F. Ogliaro, M. Bearpark, J. J. Heyd, E. Brothers, K. N. Kudin, V. N. Staroverov, R. Kobayashi, J. Normand, K. Raghavachari, A. Rendell, J. C. Burant, S. S. Iyengar, J. Tomasi, M. Cossi, N. Rega, J. M. Millam, M. Klene, J. E. Knox, J. B. Cross, V. Bakken, C. Adamo, J. Jaramillo, R. Gomperts, R. E. Stratmann, O. Yazyev, A. J. Austin, R. Cammi, C. Pomelli, J. W. Ochterski, R. L. Martin, K. Morokuma, V. G. Zakrzewski, G. A. Voth, P. Salvador, J. J. Dannenberg, S. Dapprich, A. D. Daniels, . Farkas, J. B. Foresman, J. V. Ortiz, J. Cioslowski, and D. J. Fox, "Gaussian 09 Revision D.01." Gaussian Inc. Wallingford CT 2009.
- ⁶⁰ J. T. M. Dunning, "Gaussian basis sets for use in correlated molecular calculations. I. the atoms boron through neon and hydrogen," *J. Chem. Phys.*, vol. 90, p. 1007, 1989.
- ⁶¹ M. Valiev, E. Bylaska, N. Govind, K. Kowalski, T. Straatsma, H. van Dam, D. Wang, J. Nieplocha, T. W. E. Apra, and W. de Jong, "NWChem: A comprehensive and scalable open-source solution for large scale molecular simulations," *Comput. Phys. Comm.*, vol. 181, p. 1477, 2010.
- ⁶² F. Weigend and R. Ahlrichs, "Balanced basis sets of split valence, triple zeta valence and quadruple zeta valence

- quality for H to Rn: Design and assessment of accuracy,” *Phys. Chem. Chem. Phys.*, vol. 7, p. 3297, 2005.
- ⁶³ C. Adamo, M. Cossi, G. Scalmani, and V. Barone, “Accurate static polarizabilities by density functional theory: Assessment of the PBE0 model,” *Chem. Phys. Lett.*, vol. 307, p. 265, 1999.
- ⁶⁴ K. Burke, “Perspective on density functional theory,” *J. Chem. Phys.*, vol. 136, p. 150901, 2012.
- ⁶⁵ A. J. Cohen and P. Mori-Sánchez, “Dramatic changes in electronic structure revealed by fractional charged nuclei,” *J. Chem. Phys.*, vol. 140, p. 044110, 2014.
- ⁶⁶ A. V. Sergeev, D. Z. Goodson, S. E. Wheel, and W. D. Allen, “On the nature of the Møller-Plesset critical point,” *J. Chem. Phys.*, vol. 123, p. 064105, 2005.
- ⁶⁷ M. L. Leininger, W. D. Allen, H. F. S. III, and C. D. Sherrill, “Is Møller-Plesset perturbation theory a convergent *ab initio* method?,” *J. Chem. Phys.*, vol. 112, p. 9213, 2000.
- ⁶⁸ F. H. Stillinger, “Møller-Plesset convergence issues in computational quantum chemistry,” *J. Chem. Phys.*, vol. 112, p. 9711, 2000.
- ⁶⁹ T. Janowski, K. Wolinski, and P. Pulay, “Efficient calculation of the density response function from generalized polarizabilities,” *Theor. Chim. Acta*, vol. 135, p. 6, 2016.
- ⁷⁰ P. Mori-Sánchez, A. J. Cohen, and W. Yang, “Localization and delocalization errors in density functional theory and implication for band-gap prediction,” *Phys. Rev. Lett.*, vol. 100, p. 146401, 2008.
- ⁷¹ A. J. Cohen, P. Mori-Sánchez, and W. Yang, “Challenges for density functional theory,” *Chem. Rev.*, vol. 112, p. 289, 2012.